ALMA Memo 457
Standing Waves for ALMA : simulations of various tangent cones on the subreflector

A. Bacmann (ESO)
&
S. Guilloteau (IRAM/ESO)

May 24, 2003

Abstract

The amplitude of standing waves are calculated in various subreflector geometries (subreflector with absorber, subreflector with aperture to accommodate calibration loads). The ability of scattering cones to reduce the standing waves are compared for several types of cones (straight cone, inverse straight cone within the aperture, curved cone) and cone sizes. At 3 mm, the peak-to-peak ripple due to standing waves is around 0.7% for a subreflector with absorber, which can be reduced by a factor of 9 ($\sim 0.08\%$) by fitting a straight cone on the blockage zone. The ripple is on the other hand increased to 1.4% when the subreflector presents an aperture in the blockage zone. It can further be reduced to 0.8% by fitting an inverted cone inside of the aperture. Using a curved cone instead of a straight one can only moderately improve the standing wave level.
We recommend implementing a straight cone covering somewhat more than the blockage zone. Further optimization of this parameter requires more elaborate software and should be carried out jointly with the Receiver and Antenna IPTs.

1 Introduction

At the feed horn, part of the incoming radiation is reflected back to the subreflector, generating a system of standing waves. The amplitude of the standing waves can be reduced by fitting a appropriately shaped cone over the blockage area of the subreflector. These simulations calculate the amplitude of the reflection coefficients at the subreflector for several types of cones. The abilities of the cones to reduce standing waves are compared.

This memo is mostly oriented towards astronomers, to provide them with a simple enough answer on the baseline ripple level. It only considers the on-axis reflection coefficient, and does not consider effect on the antenna gain and beam shape.

2 Geometry

2.1 Notations

In this document, we use the following notations (cf. figures below):

- Particular points
  - F: secondary focus (Cassegrain focus)
  - A: apex of the subreflector
  - O: origin of the hyperbola, middle of the segment FF', where F' is the primary focus
- Variables
  - θ: angle defining the position on the subreflector (or cone). It is measured from the secondary focus.
  - θ_0: defines the size of the cone, when there is one.
  - $r(\theta)$: distance between the focus and the position on the surface of the subreflector (or the cone) defined by the angle θ.
  - α: semi-angle of the straight cone
  - R_c: curvature radius of the curved cone
- Constants
  - L: distance between F and the apex of the subreflector A
  - e: eccentricity of the hyperbolic subreflector
  - a: distance OA
  - c: distance OF (so that $c + a = L$, and $c = e\ a$, and $a = L/(1 + e)$).
  - θ_b: the angle θ_b defines the size of the blockage zone on the subreflector
  - θ_s: defines the size of the subreflector
  - d_b: diameter of the aperture in the subreflector, which was chosen the same size as the blockage zone. The depth of the aperture was taken as $d_b + \epsilon$.

For ALMA:
$e = 1.105263$
$L = 5.883\,\mathrm{m}$
$\theta_b = 0.25°$ and $d_b = 0.051\,\mathrm{m}$
$\theta_s = 3.58°$ and $d_s = 0.750\,\mathrm{m}$ (diameter of the subreflector)

$D = 12\,\mathrm{m}$: diameter of the primary
f_p =4.8 m: focal length of the primary
$f/D = 8.0$: final f/D of telescope
$v = 0.750\,\mathrm{m}$: primary vertex hole clear aperture

Note that the value taken for θ_b is an arbitrary value slightly larger than the real blockage zone calculated for on-axis receivers (for which θ_b^{real} is $0.2238\,°$ and d_b^{real} is 22.98 mm). The diameter of the blockage zone for the actual design (off-axis receivers) will also be larger than 22.98 mm.

2.2 Studied cases

Several geometries were investigated:

1. simple hyperbolic subreflector, with and without absorber on the blockage zone

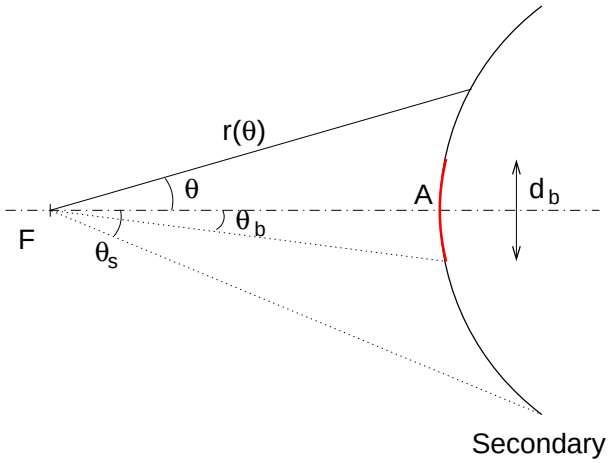

Figure 1: Simple hyperbolic subreflector. The angle (from the secondary focus) defining the blockage zone is noted θ_b, the angle defining the edge of the subreflector is θ_s, and $r(\theta)$ is the distance between the secondary focus and the point on the subreflector defined by the angle θ.

In this case, the distance $r(\theta)$ for $0 \leq \theta \leq \theta_s$ is simply given by:

$$r(\theta) = \frac{L\,(e-1)}{e\ \cos(\theta) - 1}$$

2. straight cones, tangent to the subreflector at a point defined by the angle (measured from the secondary focus) θ_0 (Fig. 2). The semi-angle of the cone α is related to θ_0 by:

$$\tan(\theta_0) = \frac{a\ (e^2-1)}{a\ \tan(\alpha) + c\sqrt{\tan^2(\alpha) - (e^2-1)}}$$

The distance $r(\theta)$ is given by:

$$0 \leq \theta \leq \theta_0 \quad : \quad r(\theta) = \frac{\sin(\alpha)}{\sin(\alpha-\theta)}\,(e\,a + a^2/x_0)$$

$$\theta_0 \leq \theta \leq \theta_s \quad : \quad r(\theta) = \frac{L\,(e-1)}{e\ \cos(\theta) - 1}$$

with

$$x_0 = \frac{a\ \tan(\alpha)}{\sqrt{\tan(\alpha)^2 - (e^2-1)}}$$

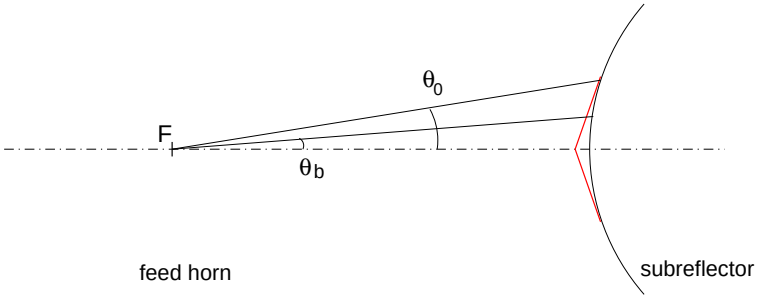

Figure 2: "Straight" cone, tangent to the subreflector at angle θ_0.

3. cones of curvature radius R_c, tangent to the subreflector at the point defined by θ_0 (Fig. 3).

   The distance $r(\theta)$ in this case is:

$$0 \leq \theta \leq \theta_0 \;:\; r(\theta) = (x_c + c)\,\cos(\theta) + y_c\,\sin(\theta) + \sqrt{[(x_c + c)\,\cos(\theta) + y_c\,\sin(\theta)]^2 - [(x_c + c)^2 + y_c^2 - R_c^2]}$$

$$\theta_0 \leq \theta \leq \theta_s \;:\; r(\theta) = \frac{L\,(e-1)}{e\;\cos(\theta) - 1}$$

   where

$$\begin{aligned} x_0 &= \frac{c\,\tan^2(\theta_0) + \sqrt{\Delta}}{e^2 - 1 - \tan^2(\theta_0)} \quad \text{with} \quad \Delta = (e^2-1)\,e^2\,\tan^2(\theta_0) + a^2\,(e^2-1)^2 \\ y_0 &= \tan(\theta_0)\,(x_0 + c) \\ x_c &= x_0 - \frac{R_c\,(e^2-1)}{\sqrt{(e^2-1) + y_0^2/x_0^2}} \\ y_c &= y_0 - \frac{R_c\;y_0/x_0}{\sqrt{(e^2-1) + y_0^2/x_0^2}} \end{aligned}$$

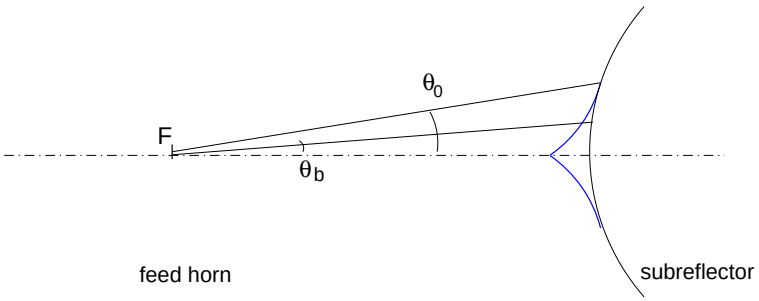

Figure 3: Cone of curvature radius R_c, tangent to the subreflector at angle θ_0.

4. hyperbolic subreflector with aperture at the blockage zone, in order to accommodate calibration devices. The bottom of the aperture retains the hyperboloidal shape of the subreflector. For simplicity in the calculation, the edges of the aperture are slightly conical (not shown on the figure), so that the diameter of the aperture is d_b at the subreflector apex, and $d_b + 2\,d_b/\sin(\theta_b)$ at the bottom of the aperture.

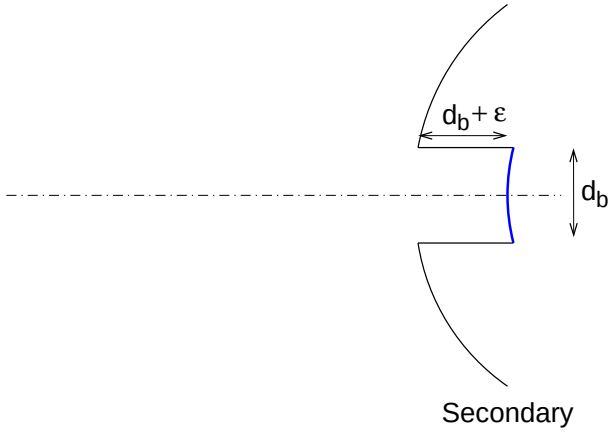

Figure 4: Hyperbolic subreflector with aperture at the blockage zone

The distance $r(\theta)$ is:

$$0 \leq \theta \leq \theta_b \quad : \quad r(\theta) = \frac{L\,(e-1)}{e\ \cos(\theta) - 1} + 2\,\frac{L\,(e-1)}{e\ \cos(\theta_b) - 1}\,\sin(\theta_b) + \epsilon$$

$$\theta_b \leq \theta \leq \theta_s \quad : \quad r(\theta) = \frac{L\,(e-1)}{e\ \cos(\theta) - 1}$$

5. hyperbolic subreflector with aperture at the blockage zone, and inverse cone in the aperture in order to reduce the standing waves arising from the discontinuity in the subreflector.

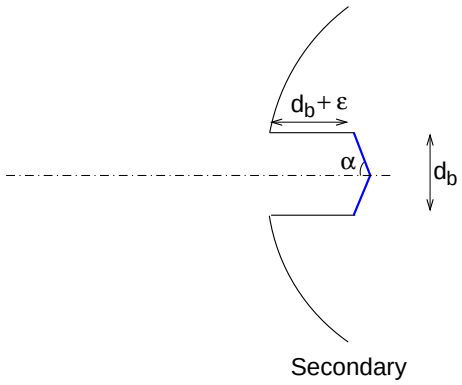

Figure 5: Subreflector with inverted cone within the aperture

The distance $r(\theta)$ is:

$$0 \leq \theta \leq \theta_b \quad : \quad \frac{\sin(\alpha)}{\sin(\alpha+\theta)} \times \left(x_b + x_c + 2\,\frac{L\,(e-1)}{e\ \cos(\theta_b) - 1}\,\sin(\theta_b) + \epsilon \right)$$

$$\theta_b \leq \theta \leq \theta_s \quad : \quad r(\theta) = \frac{L\,(e-1)}{e\ \cos(\theta) - 1}$$

with

$$x_b = \frac{L\,(e-1)}{\tan(\theta_b)[\,e\ \cos(\theta_b) - 1]} \quad \text{and} \quad x_c = \frac{\tan(\theta_b)}{\tan(\alpha)} \times \left(x_b + 2\,\frac{L\,(e-1)}{e\ \cos(\theta_b) - 1} + \epsilon \right)$$

The curvatures are exaggerated on the figures for readability.

3 Determination of reflection coefficient

The complex reflection coefficient γ is given by :

$$\gamma = \int_{subref} \Psi(\Psi^*)^* \cdot dS$$

with $\Psi = F(\theta) \cdot \exp(-jkr(\theta))$, $F(\theta)$ is the gaussian illumination function, k is the wave vector. For the calculation, a taper of 10 dB at the edge of the subreflector was chosen.

Thanks to the symmetry of the geometry, the reflection coefficient can be written (e.g. Padman & Hills 1991):

$$\gamma = \int_0^{\theta_s} 2\pi \cdot F^2(\theta) \sin(\theta) \exp(-2jkr(\theta)) d\theta$$

This expression can be asymptotically developed into:

$$\gamma = \frac{2\pi}{2jkLe(e-1)} \times [F^2(\theta_0)(e\cos(\theta_0) - 1)^2 \exp(-2jkr(\theta_0)) - F^2(\theta_s)(e\cos(\theta_s) - 1)^2 \exp(-2jkr(\theta_s))] \quad (1)$$

The first term (in θ_0) arises from the reflection at the centre of the subreflector whereas the second term (in θ_s) arises from the reflection at the edge. The interaction of these 2 terms generates an oscillation of the reflection coefficient with the wavelength. In reality, the second term will not have a large impact, since the receivers will be off-axis and the subreflector not perfectly circular. The oscillations should therefore be smaller than in the figures shown in Section 4.

From the factor in $1/k$ in Eq. 1, it can be seen that the mean value of the reflection coefficient is proportional to the wavelength. Standing waves will mostly be a problem at low frequencies.

For ALMA, the frequency of the standing waves is around 25 MHz.

4 Results

The amplitude of the reflection coefficient was calculated for the previously described geometries, as a function of the wavelength λ (λ around 3 mm), for various angles θ_0 (ie various cone sizes), and for different curvature radii of the cone in the case of a curved cone (Fig. 3). The results are presented as 3 dimensional plots[1].

Results are presented here for wavelengths around 3 mm (100 GHz). For shorter wavelengths, the amplitude of the standing waves decreases.

All calculations were performed for on-axis receivers.

4.1 Subreflector with absorber

The reference case is the simple hyperbolic subreflector, without or with an absorber covering exactly the blockage zone. The amplitude of the reflection coefficient as a function of wavelength in those 2 cases is shown in Fig. 6. As mentioned in the previous section,

[1] The Y axis carries *the opposite* of the Y coordinate for presentation reasons, so that ie $-R_c$ is plotted

the oscillation with a frequency of ∼1.2 GHz is described by the interference of both terms in Eq. (1), and the general slope arises from the wavelength proportionality.

Both cases give similar results, i.e. an average amplitude for the reflection coefficient of $4.5\,10^{-3}$ at 100 GHz.

4.2 Straight Cone

Figure 7 shows for the tangent cone on the subreflector the variation of the reflection coefficient with the wavelength and the point of tangency defined by θ_0.

The reflection coefficient drops when the cone becomes larger (and is thus tangent at larger θ_0/θ_b ratios). This decrease is about a factor of 9 for $\theta_0/\theta_b \geq 1.1$, with respect to the case without any cone (or $\theta_0 = 0$). This corresponds to a semi-angle of the cone of 87.3°. Table 1 gives the correspondence between cone semi-angle and the ratio θ_0/θ_b here chosen as parameter. Very large cones ($\theta_0/\theta_b > 1.5$) can reduce the standing waves further but represent no solution since they will also strongly modify the beam of the instrument.

Table 1: Correspondence between cone semi-angle and the ratio θ_0/θ_b in the case of a straight cone of semi-angle α, tangent on the subreflector at a position defined by the angle θ_0.

α (°)	89.5	89	88.5	88	87.5	87	86.5	86	85.5	85
θ_0/θ_b	0.21	0.42	0.63	0.84	1.05	1.26	1.48	1.69	1.90	2.11

Using a cone of $\theta_0/\theta_b = 1.1$, the average amplitude of the reflection coefficient at 100 GHz is $5\,10^{-4}$.

4.3 Cone of curvature radius R_c

Figure 8 shows the variation of the reflection coefficient with the wavelength and the point of tangency defined by θ_0 when a curved cone of curvature radius R_c is fitted on

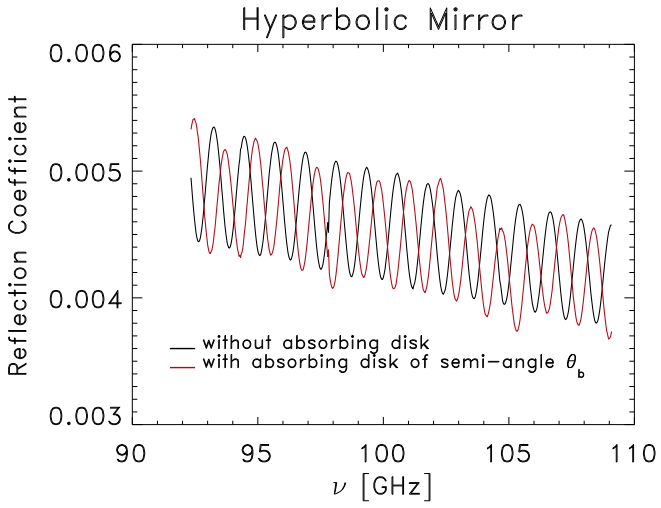

Figure 6: Reflection coefficient for a hyperbolic subreflector, with and without an absorber covering the blockage zone.

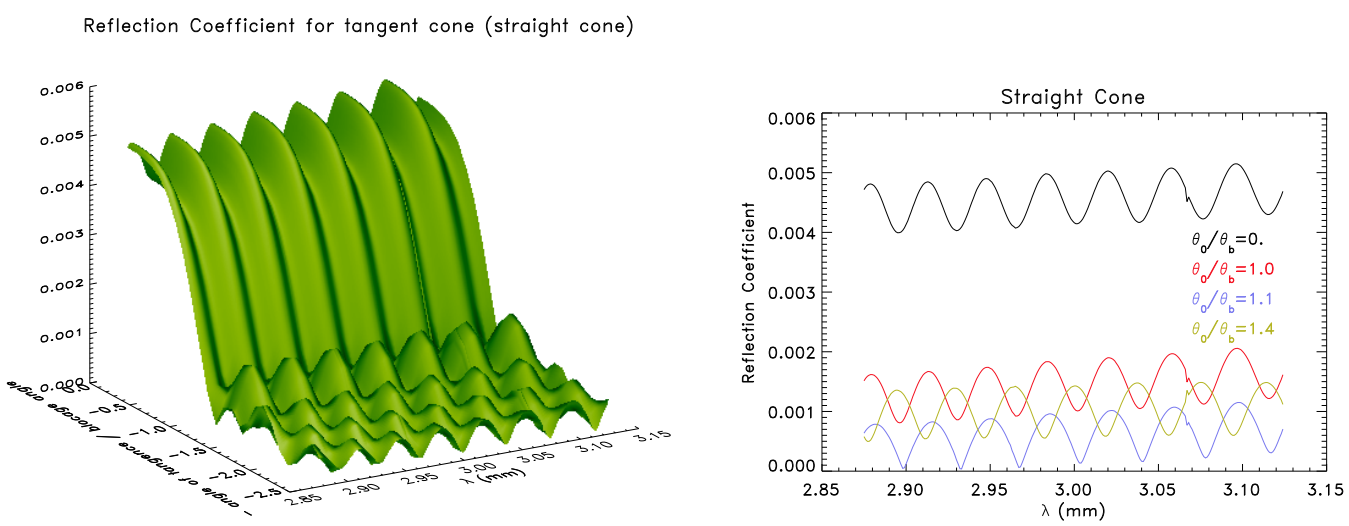

Figure 7: Straight cone of semi-angle α: reflection coefficient as a function of wavelength λ (mm) and the ratio θ_0/θ_b. *Left panel*: 3 dimensional plot showing the reflection coefficient as a function of wavelength and size of the cone (defined by the ratio θ_o/θ_b - for correspondence with the angle α, see Table 1).*Right panel*: reflection coefficient as a function of frequency for 3 sizes of cones, $\theta_0/\theta_b = 0$ ie no cone (black curve), $\theta_0/\theta_b = 1$ (red curve), $\theta_0/\theta_b = 1.1$ (blue curve), and $\theta_0/\theta_b = 1.4$ (yellow curve).

the blockage zone (same as Fig. 7 for a curved cone). The curvature radius was set to 1 m for this figure.

The variations of the reflection coefficient are very similar to the case of the straight cone. They are however not identical, and the oscillations are not in phase, which means that for the same cone size, and a fixed curvature radius, the curved cone will not always be better than the straight one (cf. § 5).

Cuts of the plot on the left panel of Fig. 8 are shown in the right panel, for $R_c = 1\,\mathrm{m}$ and 2 different wavelengths. The case of the straight cone is plotted for comparison. Fig. 8 illustrates that there is an improvement in the reflection coefficient when the cone (curved or straight) covers significantly the blockage zone. Best values are obtained for $\theta_0/\theta_b \geq 1$.

Figure 9 shows the variation of the reflection coefficient with the wavelength and the curvature radius R_c, for a ratio $\theta_0/\theta_b = 1$.

The reflection coefficient is high at low curvature radii (10 cm), and drops sharply until about $R_c \simeq 1\,\mathrm{m}$ and then evolves towards its asymptotical value. The asymptotical value is the value obtained for the straight cone of the same size (same θ_0), corresponding to an infinite curvature radius. The variations of the reflection coefficient with R_c depend on the size of the cone, as shown in Fig. 9. It also varies with the wavelength for a given cone size.

Finally, Fig. 10 shows the reflection coefficient at a given wavelength (here 3 mm) as function of the curvature radius and θ_0/θ_b. Larger cones give better results (especially for $\theta_0/\theta_b > 1$) although they will modify the primary beam and reduce the useful surface of the subreflector for $\theta_0/\theta_b > 1$. At 3 mm, cones having a curvature radius of $\simeq 1\,\mathrm{m}$ give slightly better results than straighter ones ($R_c > 1\,\mathrm{m}$), and much better results than curvier ones ($R_c < 1\,\mathrm{m}$).

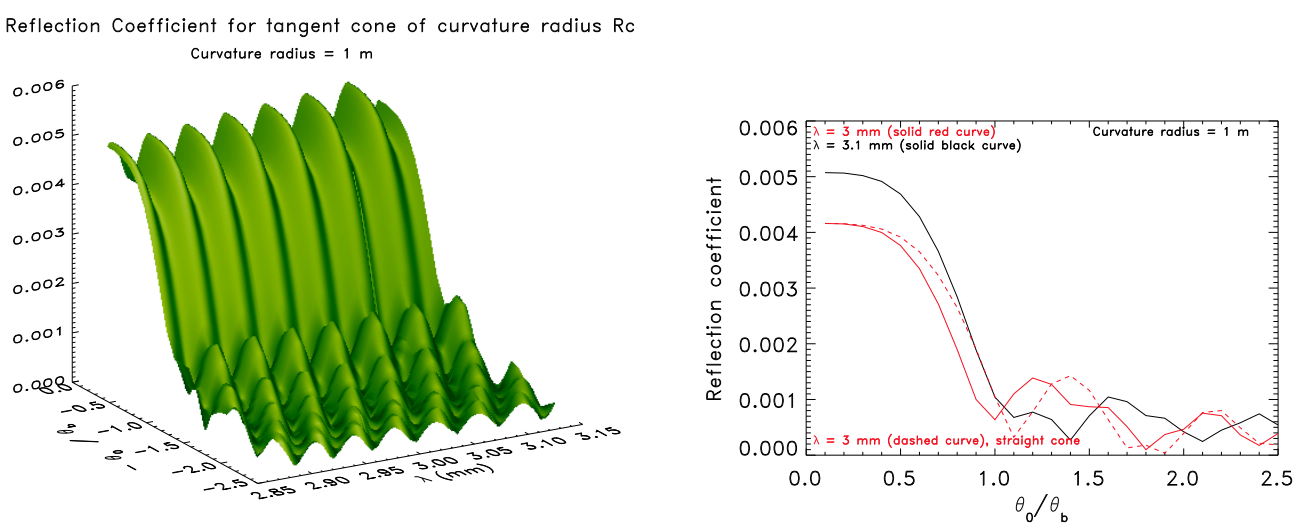

Figure 8: Reflection coefficient for a curved cone of size defined by θ_0 and curvature radius R_c. *Left panel:* 3-dimensional plot showing the reflection coefficient as a function of wavelength λ (mm) and the ratio θ_0/θ_b, for $R_c = 1\,\mathrm{m}$. *Right Panel:* reflection coefficient as a function of the ratio θ_0/θ_b, for $R_c = 1\,\mathrm{m}$ and 2 wavelengths: 3 mm and 3.1 mm. The cut for the straight cone at 3 mm is plotted for comparison (dashed line).

4.4 Subreflector with aperture

Figure 11 shows the case of a subreflector with an aperture in the central blockage zone. The depth of the aperture was chosen to be roughly equal to the diameter of the blockage zone d_b, but was allowed to vary by a fraction of the wavelength around d_b, ϵ. The effect of the aperture is to increase the reflection coefficient by about a factor of 2 with respect to the case without aperture (and without cone), to around $9\,10^{-3}$.

4.5 Subreflector with aperture and inverted cone within the aperture

Figure 12 shows the modification of the previous case when a reversed cone of semi-angle α is put in the aperture. Reversed and non-reversed cones were investigated but the results were the same (in terms of reflection coefficient, but of course not in terms of spillover). By increasing the semi-angle α of the cone, the standing waves can be reduced. In this case, the cone always has the size of the aperture when its semi-angle α is increased, therefore increasing α will not modify the antenna gain. We can then reduce the reflection coefficient at 100 GHz to about $5\,10^{-3}$.

5 Comparison Straight cone / curved cone

This section compares the reflection coefficient obtained in the case of a straight cone defined by θ_0/θ_b and a cone of curvature radius R_c of the same size (ie with the same θ_0/θ_b). Figure 13 shows this comparison for $\theta_0/\theta_b = 1$ and $\theta_0/\theta_b = 1.1$.

In the case where $\theta_0/\theta_b = 1$, the reflection coefficient is decreased with respect to the straight cone for $R_c \geq 1\,\mathrm{m}$. For a slightly larger cone ($\theta_0/\theta_b = 1.1$), the curvature radius has to be larger ($R_c \geq 2\,\mathrm{m}$) to improve the reflection coefficient of the curved cone over that of the straight cone.

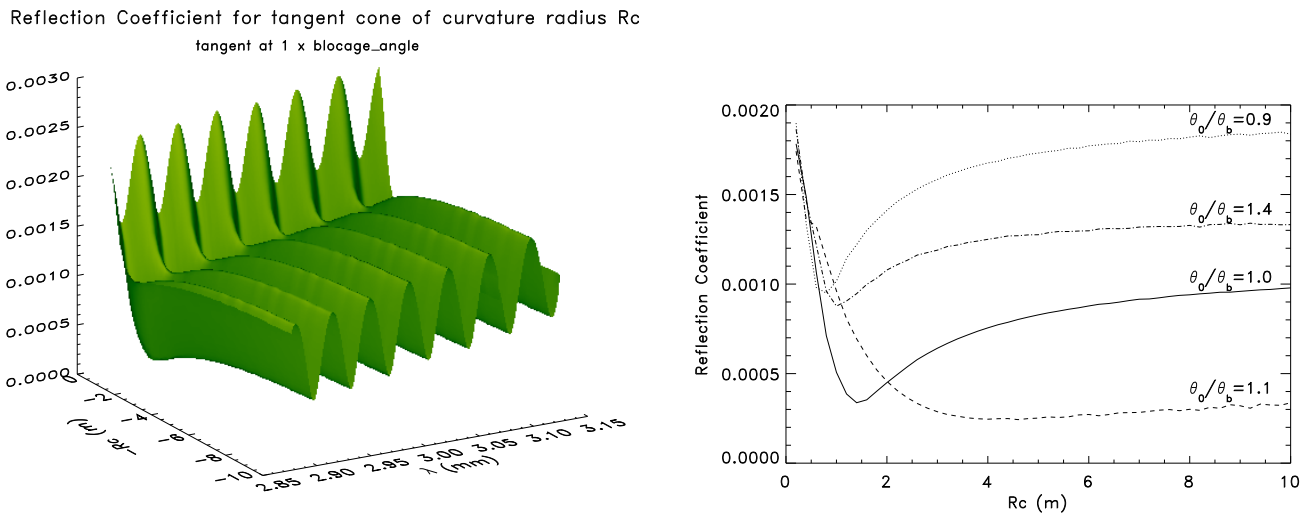

Figure 9: Curved cone: *(left panel)* - reflection coefficient as a function of wavelength λ (mm) and curvature radius R_c, for $\theta_0/\theta_b = 1$. *(right panel)* - at 3 mm, reflection coefficient as a function of R_c for different θ_0/θ_b ratios.

6 Peak-to-peak ripple

The amplitude b of the standing wave is given by :

$$b = \frac{a\, t_s}{1 - r_s\, r_m\, \exp\left(-2\pi\, \Psi\right)}$$

where a is the amplitude of the incident wave, r_s the reflection coefficient at the subreflector, r_m the reflection coefficient at the horn, and Ψ the complex illumination function of the subreflector. The voltage standing wave ratio (in power) is therefore close to $1+4\, r_s\, r_m$. In the following, we assume r_m to be 0.4.

Table 2 sums up the baseline ripple (in percentage of the baseline level) in the various geometries described in this memo. The various cases are recalled below.
- case 1: simple hyperbolic subreflector
- case 2: subreflector with straight cone
- case 3: subreflector with curved cone (of curvature radius 1.8 m)
- case 4: aperture in subreflector
- case 5: aperture in subreflector and inverted cone in aperture

For cases 2 and 3, the size of the cone is such that $\theta_0/\theta_b = 1.1$.

Table 2: Amplitude of the baseline ripple for the various geometries studied.

case 1	case 2	case 3	case 4	case 5
0.7%	0.08%	0.06%	1.4%	0.8%

These numbers show that the better design for the reduction of the standing waves is a hyperbolic mirror with a cone covering the blockage zone or a little larger ($\theta_0/\theta_b = 1.1-1.5$, angle $86.5 - 87.2°$). Because of the discontinuity at the aperture edge, designs with apertures in the subreflector are much less favorable, even with a cone within the aperture.

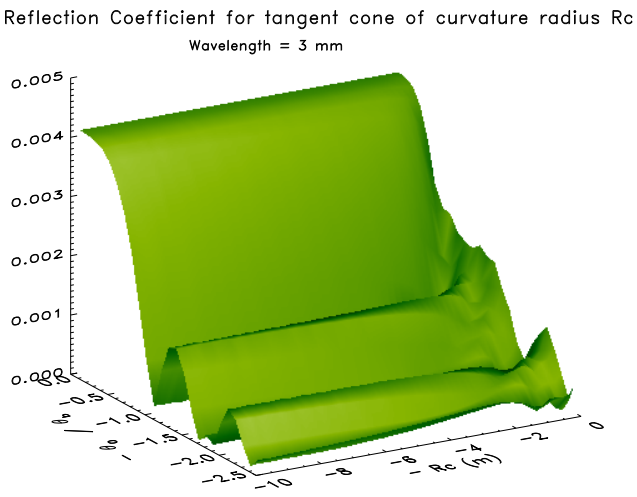

Figure 10: Curved cone: reflection coefficient as a function of curvature radius R_c and θ_0/θ_b, for $\lambda = 3\,\mathrm{mm}$.

7 Discussion and Conclusions

The figures presented above clearly show that the best solution to reduce standing waves is to provide a tangent cone to the subreflector, and that a hole should be avoided. Tangent cones larger than the blockage zone offer a better reduction in standing wave level than a cone just matching the blockage.

With a cone of radius $\theta_0 = 1.1\theta_b$, a slight improvement is further obtained by using a shaped cone with a curvature radius 1.8 m. Better results could also be obtained by using slightly larger cones. However, such further optimization should check also that the antenna gain is not significantly affected.

It is important to note that optimization of the cone shape cannot be done at a single frequency, but must be performed over a significant range. This is due to the existence of a series of local minima of the reflection coefficient. These minima occur at changing frequencies as a function of the cone shape. Instead, we must consider the worst case scenario for the standing waves, i.e. the envelope of the local maxima of the reflection coefficient as a function of frequency.

In all cases presented here, we have explored a much larger range of wavelengths (down to 0.35 mm), ensuring that the reduction obtained in the 3 mm band was not there at the expense of an increase at the higher frequencies. We found that the asymptotic behavior (coefficient $\propto \lambda$) was reached for wavelengths smaller than about 1.5 mm.

Considering manufacturing capabilities, and the fact that we have neglected a number of effects (off-axis receivers, subreflector misalignment), we recommend the adoption of a straight cone of radius $\theta_0 = 1.1 - 1.5\,\theta_b$.

Acknowledgements: we thank Richard Hills for helpful discussions and comments.

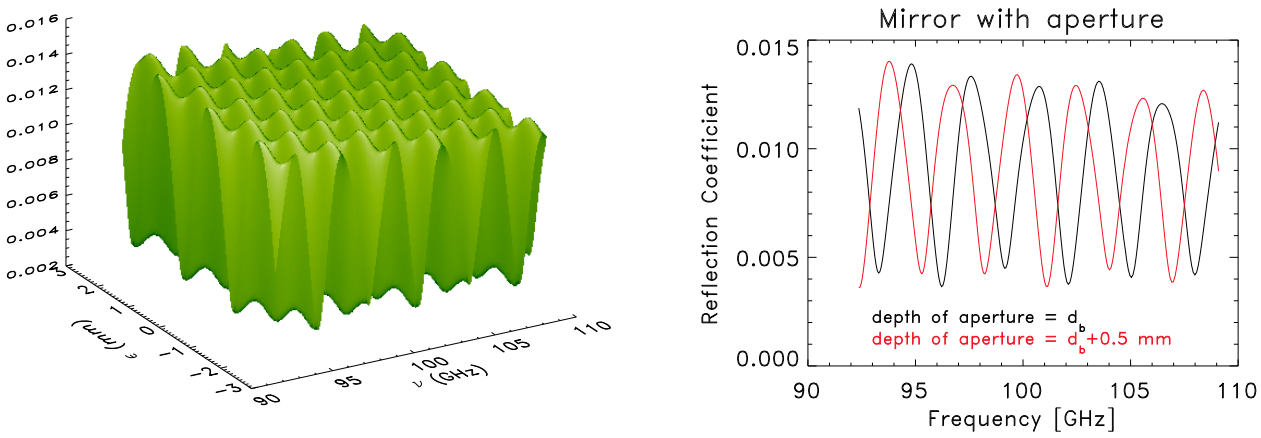

Figure 11: Reflection coefficient for a subreflector with an aperture in the blockage zone. The depth of the aperture is $d_b + \epsilon$, with ϵ a fraction of the wavelength. *Left panel:* 3 dimensional plot representing the reflection coefficient as a function of the frequency and ϵ (here ϵ varies between -2.5 and +2.5 mm). *Right panel:* Reflection coefficient as a function of frequency for $\epsilon = 0$ (black curve) and $\epsilon = 0.5$ mm (red curve).

Reference

Padman, R., & Hills, R.E. 1991, International Journal of Infrared and Millimeter Waves, Vol 12, No. 6, 589

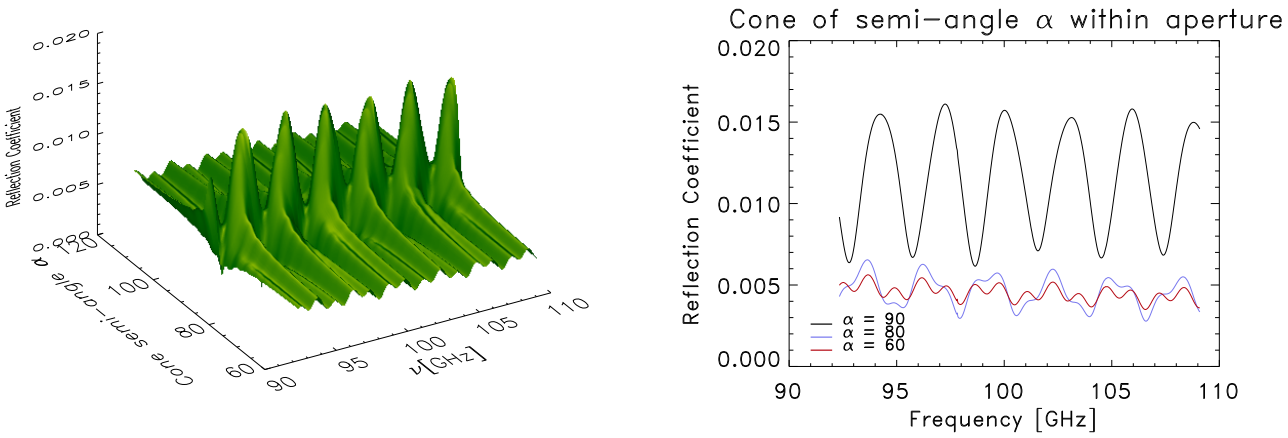

Figure 12: Reflection coefficient for a subreflector with an aperture in the blockage zone, and an inverted cone within the aperture to reduce the standing waves. The depth of the aperture is d_b. *Left panel:* 3 dimensional plot representing the reflection coefficient as a function of the frequency and the semi-angle α of the cone. *Right panel:* Reflection coefficient as a function of frequency for $\alpha = 90°$ (black curve), ie no cone, $\alpha = 80°$ (blue curve), and $\alpha = 60°$ (red curve).

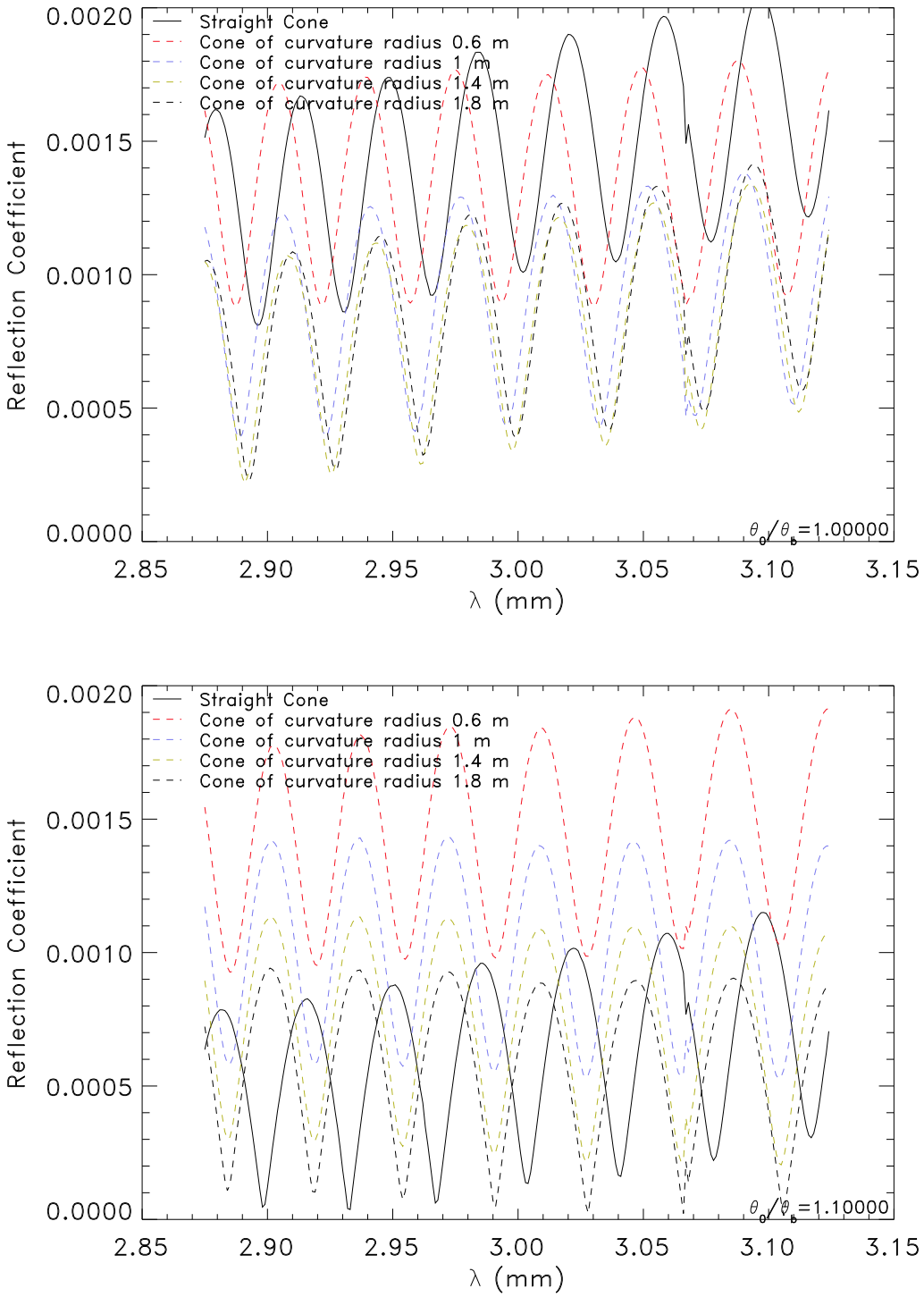

Figure 13: Comparison of the reflection coefficient for a straight cone and a cone of various curvature radii. Solid line: straight cone. Dashed lines: cone of curvature radius R_c (Red: $R_c = 0.6\,\mathrm{m}$, blue: $R_c = 1\,\mathrm{m}$, yellow: $R_c = 1.4\,\mathrm{m}$, black: $R_c = 1.8\,\mathrm{m}$). Top: $\theta_0/\theta_b = 1$. Bottom: $\theta_0/\theta_b = 1.1$.